Indoor Positioning and Navigation Methods Based on Mobile Phone Camera

Min Yu[1], Jiaohao Yu[1], Hailei Li[2], Huixia Li[2], and Hang Guo[2](✉)

[1] Jiangxi Normal University, Nanchang 330027, China
[2] Nanchang University, Nanchang 330031, China
hguo@ncu.edu.cn

Abstract. The vision technology has been used for the indoor positioning based on a mobile phone camera. In this paper, we studied the 2D positioning method by analyzing the single frame image, obtaining the camera's interior/exterior orientation parameters through the image calibration procedure, and calculating the coordinates with the homography matrix. Further, the mobile phone camera has been used for the indoor navigation. The image data is processed and converted into the mobile phone's moving distance and the attitude by the coordinate transformation method (a four-parameter fitting model), and the trajectory of the mobile phone can be calculated by the visual navigation method. In the first experiment, four points have been selected as the calibration points, and the positioning method has been conducted and analyzed. The experimental results with the software GIANT show that the error is 0.192 m in the area 9.6 m × 3.2 m, which reached a high accuracy of the indoor positioning. In the second experiment, a mobile phone has been moved inside the lab room, image data was collected, the trajectory was calculated with the navigation method proposed, and the mean error of 0.685 m has been obtained. Both results explained that the proposed methods can effectively improve the accuracy and stability of indoor positioning and navigation.

Keywords: Coordinate transformation · Homography matrix · Indoor positioning and navigation · Mobile phone localization

1 Introduction

The previous research shows that 60% of information human acquired is done through eyes. The information is so called visual information. With the continuous development of AI (Artificial Intelligence), people hope to get more and more humanoid products to serve for mankind. Therefore, computer vision arises at the historic moment. In short, computer vision is to install "eyes" on computers to simulate human visual organs. Cameras and other imaging systems are often used to simulate human eyes and provide visual information for computers. At the same time, the computer act as a human brain to process information obtained by imaging systems such as cameras, and then makes the action guidance. According to the number of cameras in the process of collecting image data, they can be divided into monocular vision, binocular vision and multi-vision.

W. Fu et al. (Eds.): ICMTEL 2021, LNICST 387, pp. 414–426, 2021.
https://doi.org/10.1007/978-3-030-82562-1_39

Therefore, positioning techniques include single frame image, double frame image, and multi-frame image method, depending on the number of image frames used.

Mobile phone localization is a method of obtaining external information through a camera. Compared with binocular and multi-visual positioning, the positioning method has the advantages of simple operation and wide applications. This technique does not need to calibrate and optimize the distance between the two cameras in binocular vision, and does not need to consider the problem of large distortion due to the different location of multiple cameras in the visual location. In computer vision, how to solve the location problem under known visual conditions has become an important research field. Mobile phone location technology can be applied to all aspects of production and life, such as target tracking, visual servoing, robot localization, etc. There are also many methods of positioning by vision techniques, such as the localization based on single-frame, double-frame, and multi-frame images. This paper mainly studied the vision localization based on the single-frame image, and the indoor navigation method based on the continue images of the mobile phone camera. The image data is processed and converted into the moving distance and the attitude of the mobile phone by the coordinate transformation (four-parameter fitting model), and the trajectory of the mobile phone can be calculated by the visual navigation method. The proposed methods can effectively improve the accuracy and stability of indoor positioning and navigation. In the future, multi-sensor navigation systems can be implemented by adding other sensors, which can further improve positioning and navigation accuracy.

2 Indoor Positioning Method Based on Single Frame Image

2.1 Visual Localization Based on Single Frame Image

Visual localization based on single-frame image is a method of locating the position information from a single image [1]. Since only one frame is used, the location process is simple, but at the same time, the amount of information contained in one frame is relatively small. Therefore, the artificial marks must be set in the environment that needs to be located. The location parameters of the marks must be known to assist the completion of the positioning process. We can use points, straight lines, and advanced geometry as artificial marks. A straight linear feature is favored by some scholars because of its advantages such as being unobstructed and easy to extract. There is little research on advanced geometric feature for localization at present since the position of geometric features needs to be solved for very complex nonlinear equations, and algorithm has very high complexity. Location algorithm based on the point feature is a classical algorithm in computer vision, and it is also called PnP (Perspective-n-Point) problem. This problem can be solved as: when the pinhole imaging model of the camera is known and the various parameters of the camera have been calibrated, and after the n landmarks of the real environment are acquired, the image coordinates of the n landmarks can be measured, and the coordinate values in the local coordinate system can be calculated by the image coordinates. With the GIANT software, the coordinates of these n landmarks in the local coordinate system can be calculated through the coordinates of the landmarks in the image coordinate system. Four points have been set as the reference points. The location errors can be obtained by comparing the calculated coordinates of the same points with the known reference coordinates.

In this paper, four points were selected as reference points (the local coordinates of the four points in the scene and the image coordinates in the pictures are all known) to calibrate the camera, and to obtain the internal and external orientation parameters as well as the distortion parameters in the camera. By using the geometric correspondence between image points and real locations in the photography, the coordinates of all points on the picture can be used to calculate the coordinates in the local coordinate system by means of the photogrammetry collinear equation. How to match the real locations with the image points is the focus of this paper. The method proposed has the advantages of simple form, convenient calculation and high accuracy.

2.2 Camera Model

The images used in the experiment were obtained by the mobile phone camera. Therefore, we need to study the characteristics and pinhole imaging model of the camera [2].

The pinhole imaging model, also known as the linear camera model, is derived from the principle of pinhole imaging, and is a linearized geometric model. The model does not consider the distortion of the camera, which is the best approximation of the actual camera. The Fig. 1 shows the camera coordinate system (*Xc, Yc, Zc*) and the world coordinate system (*Xw, Yw, Zw*), where *O* is the camera center, O_1 the focal length, and *Zc* is the optical axis of the camera which is perpendicular to the plane of the image.

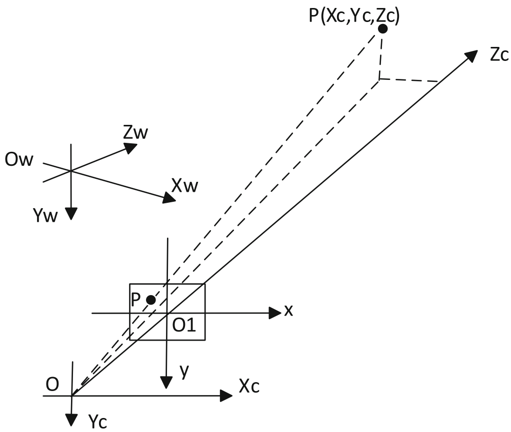

Fig. 1. Camera and the world coordinate systems

Suppose there is a point P in the real world (Fig. 1), and its coordinates in the camera coordinate system are (*Xc, Yc, Zc*), and the image coordinates of the corresponding points on the image are (*x, y*), and *f* is the focal length of the camera. The proportional relation is:

$$\begin{cases} x = \frac{f \cdot X_c}{Z_c} \\ y = \frac{f \cdot Y_c}{Z_c} \end{cases} \tag{1}$$

The above perspective projection relation is represented by the homogeneous coordinates and matrices.

$$Z_c \begin{bmatrix} x \\ y \\ 1 \end{bmatrix} = \begin{bmatrix} f & 0 & 0 & 0 \\ 0 & f & 0 & 0 \\ 0 & 0 & 1 & 0 \end{bmatrix} \begin{bmatrix} X_c \\ Y_c \\ Z_c \\ 1 \end{bmatrix} = P \begin{bmatrix} X_c \\ Y_c \\ Z_c \\ 1 \end{bmatrix} \tag{2}$$

Where Z_c is a scale factor also, and P is a perspective projection matrix. The pixel coordinates into the formula can be obtained.

$$\begin{aligned} Z_c \begin{bmatrix} u \\ v \\ 1 \end{bmatrix} &= \begin{bmatrix} \frac{1}{dx} & 0 & u_0 \\ 0 & \frac{1}{dy} & v_0 \\ 0 & 0 & 1 \end{bmatrix} \begin{bmatrix} f & 0 & 0 & 0 \\ 0 & f & 0 & 0 \\ 0 & 0 & 1 & 0 \end{bmatrix} \begin{bmatrix} R & T \\ 0^T & 1 \end{bmatrix} \begin{bmatrix} X_w \\ Y_w \\ Z_w \\ 1 \end{bmatrix} \\ &= \begin{bmatrix} a_x & 0 & u_0 & 0 \\ 0 & a_y & v_0 & 0 \\ 0 & 0 & 1 & 0 \end{bmatrix} \begin{bmatrix} R & T \\ 0^T & 1 \end{bmatrix} \begin{bmatrix} X_w \\ Y_w \\ Z_w \\ 1 \end{bmatrix} = M_1 M_2 X_w = M \begin{bmatrix} X_w \\ Y_w \\ Z_w \\ 1 \end{bmatrix} \end{aligned} \tag{3}$$

Where the rotation matrix R is the orthogonal unit matrix (3 × 3) and T is a three-dimensional translation vector, the pixel coordinates are u and v in the pixel coordinate system, the physical scales of each pixel in the direction of the x axis and the y axis are dx, dy, $a_Z = f/dx$ is the scaling factor of the u axis, $a_y = f/dy$ is the scaling factor of the v axis, M is the projection matrix, and the M_1 is the directional parameter within the camera. M_2 is the orientation parameter of the camera, and it is determined by the orientation of the camera relative to the local coordinate system. When the camera's internal and external parameters are known, that is, the projection matrix M is known. For any spatial point $P_w(X_w, Y_w, Z_w)$, the coordinates x, y of its image point $p(u, v)$ can be obtained.

2.3 Principle of Image Measurement

According to the principle of the photography, the homography matrix is satisfied between the scene plane and the image plane [3–5]. First, we need to obtain the homography matrix H, and then can calculate the coordinates of all points in the scene plane based on that of the image plane. Suppose that the homography matrix is:

$$H = \begin{bmatrix} H_{11} & H_{12} & H_{13} \\ H_{21} & H_{22} & H_{23} \\ H_{31} & H_{32} & H_{33} \end{bmatrix} \tag{4}$$

And

$$h = (H_{11}, H_{12}, H_{13}, H_{21}, H_{22}, H_{23}, H_{31}, H_{32}, H_{33})^T \tag{5}$$

$$x_P^{'} = \left(x_1^{'},\ y_1^{'},\ 1\right)^T \tag{6}$$

$$X_P = (X_1, Y_1, 1)^T \tag{7}$$

So

$$M_H(X) = \begin{bmatrix} x^T 0^T - X_1 x^T \\ 0^T x^T - Y_1 x^T \end{bmatrix} h = 0 \tag{8}$$

where $x_P^{'} = \left(x_1^{'}, y_1^{'}, 1\right)^T$ is the coordinates of any point on the image, and $X_P = (X_1, Y_1, 1)^T$ is the coordinates in the scene. According to the form of the homography matrix, we need the four known points to solve the parameter values in the homography matrix. The basic requirement of the four known points is that the coordinates in the local coordinates and the image coordinates are all known, and these points must have a general position, that is, any three points are not collinear. The locations of these points selected are shown in Fig. 2.

The results of this experiment were obtained by using GIANT software (the copyright belongs to the Mr. Clifford Mugnier of the Louisiana State University, the USA). A similar homography algorithm is used in the GIANT [6-20].

$$\begin{cases} X_w = \frac{a_1x+a_2y+a_3}{c_1x+c_2y+1} \\ Y_w = \frac{b_1x+b_2y+b_3}{c_1x+c_2y+1} \end{cases} \tag{9}$$

Based on the image plane coordinates of any point w for (x, y), by the homography matrix, one can calculate the coordinates of the point w in the local coordinates (*Xw*, *Yw*).

3 Indoor Navigation Method Based on Monocular Vision

According to the coordinate transformation method, the translation and rotation between two coordinate systems can only be calculated from the three same points on those two coordinate systems, which are non-collinear. The monocular camera can obtain the pixels of the pictures on a two-dimensions pixel coordinate system. Then, the translation and rotation between two continue coordinate systems can be fitted and determined by four parameters. The matrix algorithm is as follows [15–39]:

$$\begin{bmatrix} \mathrm{x}_2 \\ \mathrm{y}_2 \end{bmatrix} = \begin{bmatrix} \Delta \mathrm{x} \\ \Delta \mathrm{y} \end{bmatrix} + \mathrm{k} \begin{bmatrix} \cos\theta & -\sin\theta \\ \sin\theta & \cos\theta \end{bmatrix} \begin{bmatrix} \mathrm{x}_1 \\ \mathrm{y}_1 \end{bmatrix} \tag{10}$$

where $x_1,\ y_1$ are the pixel coordinates at one time point, $x_2,\ y_2$ are the pixel coordinates at next time point, $\Delta x,\quad \Delta y$ are the translation components when the mobile phone from the point 1 to the point 2, θ is the rotation between two consecutive coordinate systems, k is the scale factor between them. Set $C = kcos\theta,\quad S = ksin\theta$, and make the formula (10) expansion, one can get the formulas:

$$\begin{cases} \Delta x + x_1 {*} C - y_1 {*} S = x_2 \\ \Delta y + x_1 {*} S + y_1 {*} C = y_2 \end{cases} \tag{11}$$

or can be expressed as the following matrix formula:

$$AX = B \tag{12}$$

where $A = \begin{bmatrix} 1 & 0 & x_1 & -y_1 \\ 0 & 1 & y_1 & x_1 \end{bmatrix}$ $X = \begin{bmatrix} \Delta x \\ \Delta y \\ C \\ S \end{bmatrix}$ $B = \begin{bmatrix} x_2 \\ y_2 \end{bmatrix}$

Through the matrix solution, one can obtain the values of the matrix X, and get the translation Δx, Δy, and using C, S can calculate the rotation parameter θ as follows [40–41]:

$$\theta = arcsin\frac{S}{C*sqr\left(1+\frac{S}{C}^2\right)} \tag{13}$$

4 First Experimental Design and Data Analysis

4.1 Processing of the Feature Points

The horizontal location (two-dimensions) test was conducted inside the building of the institute on the campus as shown in the Fig. 2. The experimental site was in the indoor corridor of the institute building, and the local coordinate system of the corridor was established before the experiment, so that all the coordinates of the points in the corridor can be calculated by the local coordinate system.

Fig. 2. The experiment site with the points on the floor.

The total of 32 points in the place of the experiment are marked as the Fig. 2, including four known points (See the black points for calibrating the coefficients in the homography matrix). Due to the influence of the camera angle, these 32 points cover the length of 9.6 m and the width is 3.2 m area. The selected points are named 0–31 respectively, in and 0–3 points are selected as the known points (the black points) to

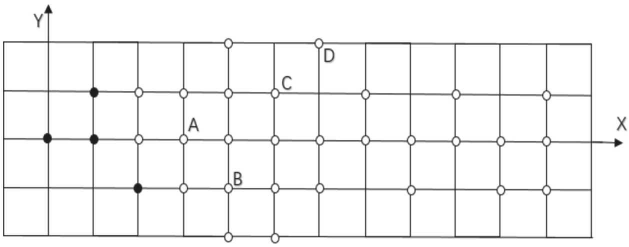

Fig. 3. The point positions in the experiment

solve the homography matrix H. The local coordinates of the remaining 28 points are obtained by the software GIANT, and the coordinates of the points are shown in the hollow points in Fig. 3.

For the purpose of checking the accuracy of the proposed method, several points were selected to calculate and compare the actual coordinates to get their errors (See points A, B, C, and D as the Fig. 3). The maximum error of the four points listed in Table 1 is 0.10 m, and the experimental error was within the allowable range.

Table 1. Comparison of partial point coordinates (Unit: m)

Selected points	Image coordinates (x, y)/pixel	Local coordinates (X, Y)	Calculated coordinates (X, Y)	Point errors (X, Y)
A	(148.24, 0.00)	(2.40,0.00)	(2.40,0.00)	(0.00,0.00)
B	(164.80, −36.50)	(3.20, −0.80)	(3.27, −0.83)	(0.07, −0.03)
C	(175.04, 30.98)	(4.00, 0.80)	(4.06, 0.81)	(0.06, 0.01)
D	(183.28, 54.18)	(4.80, 1.60)	(4.90,1.64)	(0.10, 0.04)

4.2 Analysis of Experimental Results

The result of experimental data is obtained by GIANT software. In order to show the experimental results more intuitively, Table 2. calculated the absolute error values of some points.

It can be seen from the Table 2. that the error obtained from the point (2.40, 0.00) is (0.00, 0.00), the absolute error obtained from the point (3.20, −0.80) is (0.05, 0.01), and the mean location error $\sqrt{\Delta x^2 + \Delta y^2}$ is 0.192 m in the area of 9.6 m × 3.2 m. From the error values of these points, the position closer to the origin point is very accurate, and with the distance gradually increases the error obtained is increase. The reason is that with the distance from the origin increases the distortion of the camera becomes larger, the sharpness of the image decreases, and the difficulty of finding the target point increases, which leads to an increase in calculation error.

Table 2. Absolute errors (unit: m)

True coordinates (*x*, *y*)	Measured coordinates (*x*, *y*)	Errors (△*x*, △*y*)
(2.40, 0.00)	(2.40, 0.00)	(0.00, 0.00)
(3.20, −0.80)	(3.25, −0.81)	(0.05, 0.01)
(4.00, 0.80)	(4.06, 0.81)	(0.06, 0.01)
(4.80, 1.60)	(4.88, 1.64)	(0.08, 0.04)
(5.60, 0.80)	(5.70, 0.83)	(0.10, 0.03)
(6.40, −0.80)	(6.55, −0.83)	(0.15, 0.03)
(7.20, 0.80)	(7.50, 0.83)	(0.30, 0.03)
(8.00, −0.80)	(8.56, −0.85)	(0.56, 0.05)
(8.80, 0.00)	(9.20, 0.05)	(0.40, 0.05)

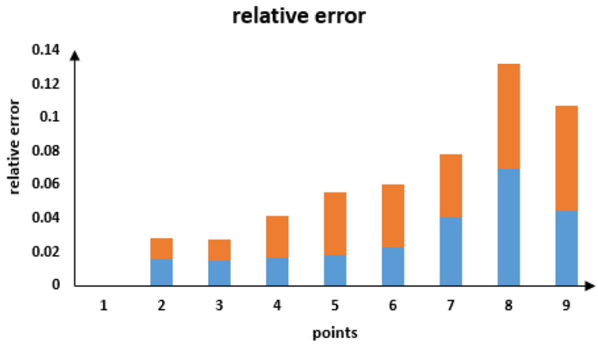

Fig. 4. Relative errors (Unit: m)

Figure 4. is the relative error on the axis *X* and *Y* coordinates. The blue color represents the *X* axis, and the orange represents the *Y* axis. As can be seen from the figure, the error on both coordinate axes gradually increases with the increase of the distance, and the increase of the two is equivalent.

4.3 Error Analysis and Improvement Measures

With the increasing of the distance from the center of the camera, the accuracy of the point solution decreases. The reasons of reducing the location accuracy are as follows:

Camera distortion is one of the reasons. The experimental basis of this paper is based on the ideal model of camera, pinhole imaging. The imaging system ignores the effect of camera distortion on the image. When the distance from the center of the camera is close, the distortion of the camera is low, and the effect on the image is very small. However, with the distance from the origin is lengthened, the influence of camera distortion on the image increases gradually, which caused positioning errors.

The errors after the initial calibration cannot be eliminated completely. It is more difficult to obtain the location accurately with the software, and the deviation gets larger and larger.

The clarity of the image is reduced, when the distance is closer to the center of the camera, it is very easy to find the location of the points when processing the pictures. However, when the distance becomes longer, it is difficult to find the points, and the recognition degree of fixed-point decreases.

5 Second Experimental Design and Data Analysis

The experiment was performed inside the XIANSU building at the campus Yao lake of Jiangxi Normal University, Nanchang, China. As shown in the Fig. 5, the test area is about 12 m × 13 m, including some sofas, tables, and the office staffs. In the experiment, a mobile phone has been used for conducting the indoor navigation. The trajectory is shown in the red line with the start of a circle and the end of a triangle.

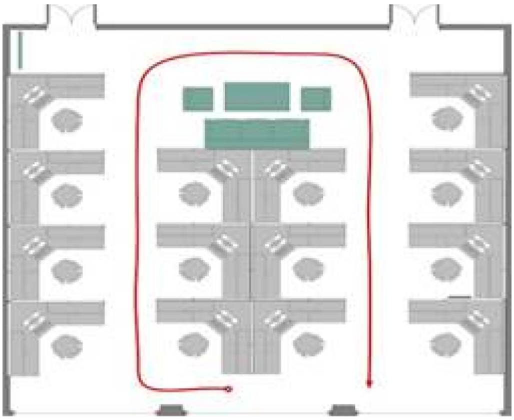

Fig. 5. Experimental trajectory

The Fig. 6 described the mobile phone test results with the green line, which compared with the real trajectory with the red line. The mean error of indoor navigation in the area of 12 m × 13 m is 0.685 m. The feature points are extracted and the processing environment is as shown in the Fig. 7.

Compared to the mobile phone positioning experiment results on the corridor at the section IV, both positioning and navigation results are shown in the Table 3. Through the two experiments, we obtained the valuable experience that a decimeter accuracy of localization and navigation can be reached with the current mobile phone camera and the methods we proposed.

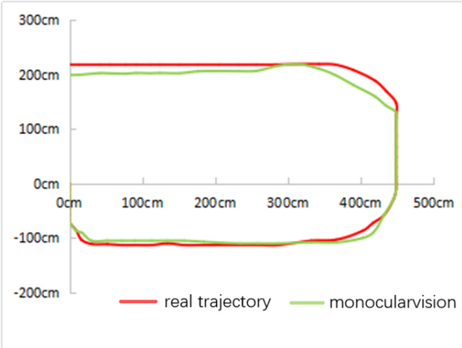

Fig. 6. Comparison of the experimental trajectory

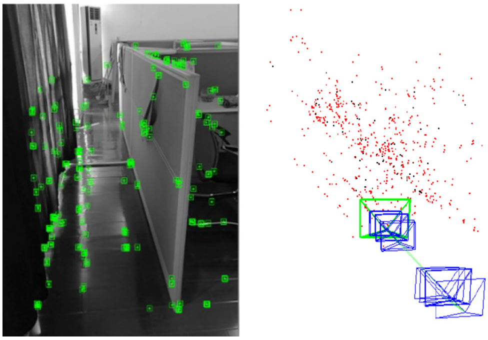

Fig. 7. Monocular visual navigation experiment

Table 3. Mobile phone location errors (unit: m)

Methods	First experiment	Second experiment
Mean errors	0.192	0.685

6 Conclusion

In this paper, the location of any point on the corridor is realized on the basis of the single-frame image. Based on the known camera model and the homography matrix, the location method based on the point feature is adopted. The first experiment proves that the method has high positioning accuracy (the mean error is 0.192 m), but it also has the shortcoming of the positioning precision decline with the distance increasing from the center of the camera. To deal with this deficiency, the reasons for the errors are analyzed, and these errors come from the distortion of the camera due to the single-frame. In the second experiment, the indoor navigation method with the mobile phone used the coordinate transformation, calculated the trajectory, and achieved the accuracy at the level of 0.685 m. In the future, when some other sensors, such as IMU, Lidar, etc., are added to conduct a multi-sensor navigation system the accuracy of positioning and navigation is expected to be improved.

Acknowledgments. The paper was supported by the projects of the National Key R&D Program of China (No. 2016YFB0502204), National Natural Science Foundation of China (No. 41764002), and the corresponding author is Prof. Hang Guo, hguo@ncu.edu.cn.

References

1. Brito, J.H., Angst, R., Köser, K., et al.: Radial Distortion Self-Calibration, Computer Vision and Pattern Recognition, pp. 1368–1375. IEEE, June 2013
2. Bukhari, F., Dailey, M.N.: Automatic radial distortion estimation from a single image. J. Math. Imaging Vis. **45**(1), 1–45 (2013)
3. Fischler, M.A., Bolles, R.C.: Random sample consensus: a paradigm for model fitting with applications to image analysis and automated cartography. Commun. ACM **24**, 381–395 (1981)
4. Fiore, P.D.: Efficient linear solution of exterior orientation. IEEE Trans. Pattern Anal. Mach. Intell. **23**(2), 140–148 (2011)
5. Shi, B., Matsushita, Y., Wei, Y., Xu, C., Tan, P.: Self-calibrating photometric stereo. In: IEEE Conference on computer vision and pattern recognition (CVPR) - San Francisco, CA, USA (2010.06.13-2010.06.18), pp. 1118–1125 (2010)
6. Schweighofer, G., Pinz, A.: Robust pose estimation from a planar target. IEEE Trans. Pattern Anal. Mach. Intell. **28**(12), 2024–2030 (2006)
7. Strobl,K.H., Hirzinger,G.: More accurate pinhole camera calibration with imperfect planar target. IEEE Int. Conf. Comput. Vis. Workshops 1068–1075 (2011)
8. Ma, S.D., Zhang, Z.Y.: Computer Vision-The Theory of Computer and Basis of Algorithm. Science Press, China (1997)
9. Kuthirummal, S., Jawahar, C.V., Narayanan, P.J.: Planar shape recognition across multiple views. Int. Conf. Patt. Recogn. **1**, 456–459 (2002)
10. Kukelova, Z., Pajdla, T.: A minimal solution to radial distortion autocalibration. IEEE Trans. Pattern Anal. Mach. Intell. **33**(12), 2410–2422 (2011)
11. Jain, P.K., Jawahar, C.V.: Homography estimation from planar contours. In: The Third International Symposium on 3D Date Processing Visualization and Transmission, pp. 877–884 (2006)
12. Kanatani, K., Ohta, N., Kanazawa, Y.: Optimal homography computation with a reliability measure. In: IAPR workshop on Machine Vision Applications, pp. 426–429 (1998)
13. Liu, R., Ruan, Z.C., Wei, S.: Algorithm research on monochronous matrix in plane measurement. J. Syst. Simul. **13**(suppl.), 174–176 (2011)
14. Wang, Y.X., Ma, Y., Chen, Q.X.: A method of line matching based on feature points. J. Softw. **7**(7), 1539–1545 (2012)
15. Xu, D., Tan, M., Li, Y.: Robot Vision Measurement and Control. National Defense Industry Press, China (2008)
16. Xu, D., Tan, M., Li, Y.: Visual Measurement and Control for Robots. National Defense Industry Press, China, pp. 35–39 (2011)
17. Liu, R., Wei, S.: Research on plane Measurement method based on Image. M.S. thesis, Elect. Inf. Eng., University of Anhui, Anhui, China (2002)
18. Han, Y.X., Zhang, Z.C., Dai, M.: Monocular vision measurement method for target ranging. Opt. Precis. Eng. **19**(5), 1110–1117 (2011)

19. Hartley, R., Zisserman, A.: Multiple View Geometry in Computer Vision: Camera Models. Cambridge University Press, vol. 30 (9–10), pp. 1865–1872 (2004)
20. Zhang, Y., Liu, Y.: Closed-from solution for circle pose estimation using binocular stereo vision. Electron. Lett. **44**(21), 1246–1247 (2008)
21. Zhang, Q.D., Fan, J.S.: Application and development of satellite navigation and positioning technology in China. J. Navig. Positioning **4**(3), 82–88 (2016)
22. Dwiyasa, F., Lim, M.H.: A survey of problems and approaches in wireless-based indoor positioning. In: International Conference on Indoor Positioning and Indoor Navigation, pp. 1–7. IEEE (2016)
23. Di, K.C., Wan, W.H., Zhao, H.Y., et al.: Progress and applications of visual SLAM. Acta Geodaetica et Cartographica Sinica **47**(6), 770–779 (2018)
24. Li, H.X., Wen, X., Guo, H., et al.: Research into Kinect/Inertial Measurement Units Based on Indoor Robots. Sensors **18**(3), 839 (2018)
25. Chen, X.L.: Research of attitude calculation of single camera visual system. Chin. J. Sci. Instrument **35**(S1), 45–48 (2014)
26. Feng, K.Q., Li, J., Zhang, X.M., et al.: A new quaternion-based Kalman filter for real-time attitude estimation using the two-step geometrically-intuitive correction algorithm. Sensors **17**(9), 2146 (2017)
27. Song, H.H., Yu, G.X., Qu, Y.B.: Monitoring and forecasting system for ship attitude motion based on extended Kalman filtering algorithm. J. Chin. Inertial Technol. **26**(1), 6–12 (2018)
28. Li, J., et al.: High-precision attitude measurement algorithm based on complementary filtering and Kalman filtering. J. Chin. Inertial Technol. **26**(1), 51–55+86 (2018)
29. Mu, X.F., Chen, J., Zhou, Z.X., et al.: accurate initial state estimation in a monocular visual – inertial SLAM system. Sensor **18**(2), 506 (2018)
30. Feng, G., Huang, X.: Observability analysis of navigation system using point-based visual and inertial sensors. Optik – Int. J. Light Electron Opt. **125**(3), 1346–1353 (2014)
31. Guo, H., Li, H., Xiong, J., Yu, M.: Indoor positioning system based on particle swarm optimization algorithm. Measurement **134**, 908–913 (2019)
32. Guo, H., Tian, B.L., Yu, M., Deng, L.K., Wang, H.T.: Improved ambiguity searching method of ultra-short baseline with nonlinear constraint. In: Proceedings of the 2018 International Technical Meeting of the Institute of Navigation, Reston, Virginia, pp. 46–55 (2018)
33. Guo, H., Uradzinski, M.: The usability of MTI IMU sensor data in PDR indoor positioning. In: 2018 25th Saint Petersburg International Conference on Integrated Navigation Systems (ICINS 2018), May 2018
34. Xu, Y., Ahn, C.K., Shmaliy, Y.S., et al.: Adaptive robust INS/UWB-integrated human tracking using UFIR filter bank. Measurement **123**, 1–7 (2018)
35. Xu, Y., Shmaliy, Y.S., Li, Y., Chen, X., Guo, H.: Indoor ins/lidar-based robot localization with improved robustness using cascaded fir filter. IEEE Access **7**(1), 34189–34197 (2019)
36. Xu, Y., Tian, G., Chen, X.: Enhancing INS/UWB integrated position estimation using federated EFIR filtering. IEEE Access **6**, 64461–64469 (2018)
37. Xu, Y., Karimi, H.R., Li, Y.Y., Zhou, F.Y., Bu, L.L.: Real-time accurate pedestrian tracking using EFIR filter bank for tightly coupling recent inertial navigation system and ultra-wideband measurements. Proc. Inst. Mech. Eng. Part I-J. Syst. Control Eng. **232**(4), 464–472 (2018)
38. Xu, Y., Chen, X.: Online cubature Kalman filter Rauch–Tung–Striebel smoothing for indoor inertial navigation system/ultrawideband integrated pedestrian navigation. Proc. Inst. Mech. Eng. Part I-J. Syst. Control Eng. **232**(4), 390–398 (2018)
39. Xu, Y., Shmaliy, Y.S., Li, Y., Chen, X.: UWB-based indoor human localization with time-delayed data using EFIR filtering. IEEE Access **5**(1), 16676–16683 (2017)

40. Uradzinski, M., Guo, H., Mugnier, C.: Checking the accuracy of an inertial-based pedestrian navigation system with a drone. GPS World **28**(6), 58–64 (2017)
41. Uradzinski, M., Guo, H., Liu, X., Yu, M.: Advanced indoor positioning using Zigbee wireless technology. Wireless Pers. Commun. **97**(4), 6509–6518 (2017). https://doi.org/10.1007/s11277-017-4852-5